Supplementary Material to Camera Pose Estimation Using First-Order Curve Differential Geometry, ECCV 2012

Complement to ECCV – Draft

1 Overview of this document

In Section 2 we present additional results for *(i)* our synthetic experiments, first clarifying the plot shown in the paper, Figure 1, and then using bundle adjustment, Figures 2–3, together with *(ii)* results for the standard Dino sequence from the Middlebury multiview stereo dataset [1], Figure 4. In the remaining sections of this document we supply additional details in the proofs of theorems and propositions from the paper. All references to equations and figures are to objects in the present document unless otherwise stated.

2 Additional Results

2.1 Synthetic experiments

Figure 1 clarifies Figure 9 of the paper, by splitting it into two plots, one for fixed tangential perturbation (top), and another for fixed positional perturbation. We also ran bundle adjustment on top of our RANSAC results, which is standard practice in applications, and recorded the distribution of reprojection errors, shown in Figures 2–3.

2.2 Dino sequence

Results: We also tested the proposed method on the standard Dino sequence from the Middlebury multiview stereo dataset [1], Figure 4. The Cameras sample 363 views at 640×480 on a hemisphere around the object. The data is low resolution compared to our Capitol dataset. The calibration accuracy in this case is hard to determine objectively, but it is "on the order of a pixel" or about 1-2px according to the authors (see a description of the calibration process below). We note that even though this is a carefully constructed dataset, the average reprojection error using our method are $1.03px$ and $0.66px$ before and after bundle adjustment, respectively, while the average error using the dataset camera is $0.88px$. This was obtained as follows. As for the Capitol sequence, we picked a set of manual edge correspondences (in this case 10) across 3 views, and reconstructed a 3D cloud of edges from the first two views using the dataset cameras. This gives a set of 3D-2D correspondences with which we seek to determine the pose of the third view and compare to the dataset pose. The third view plays the role of novel views to be iteratively integrated and registered/calibrated by a structure from motion system. We added 50% outliers to the set of manual correspondences, in order to be realistic, and ran RANSAC to select two point-tangents giving the pose which is most consistent with the data. Bundle adjustment can then be optionally run to refine this pose. The distributions of reprojection error before and after bundle adjustment, as compared to that of the dataset camera, are shown in Figure 1.

Details of the dataset calibration process: We note that the dataset calibration of the Dino sequence was performed as follows [1]: the images were captured using the Stanford Spherical Gantry which enables moving a camera on a sphere. To calibrate the cameras, they took images of a planar grid from 68 viewpoints and used a combination of Jean-Yves Bouguet's Matlab toolbox and their own software to find grid points and estimate camera intrinsics and extrinsics. From these parameters, they computed the gantry radius and camera orientation, hence enabling a map of any gantry position to camera parameters. The authors then scanned the object from several orientations using a laser scanner and merged the results. The cameras were then aligned with the resulting mesh.

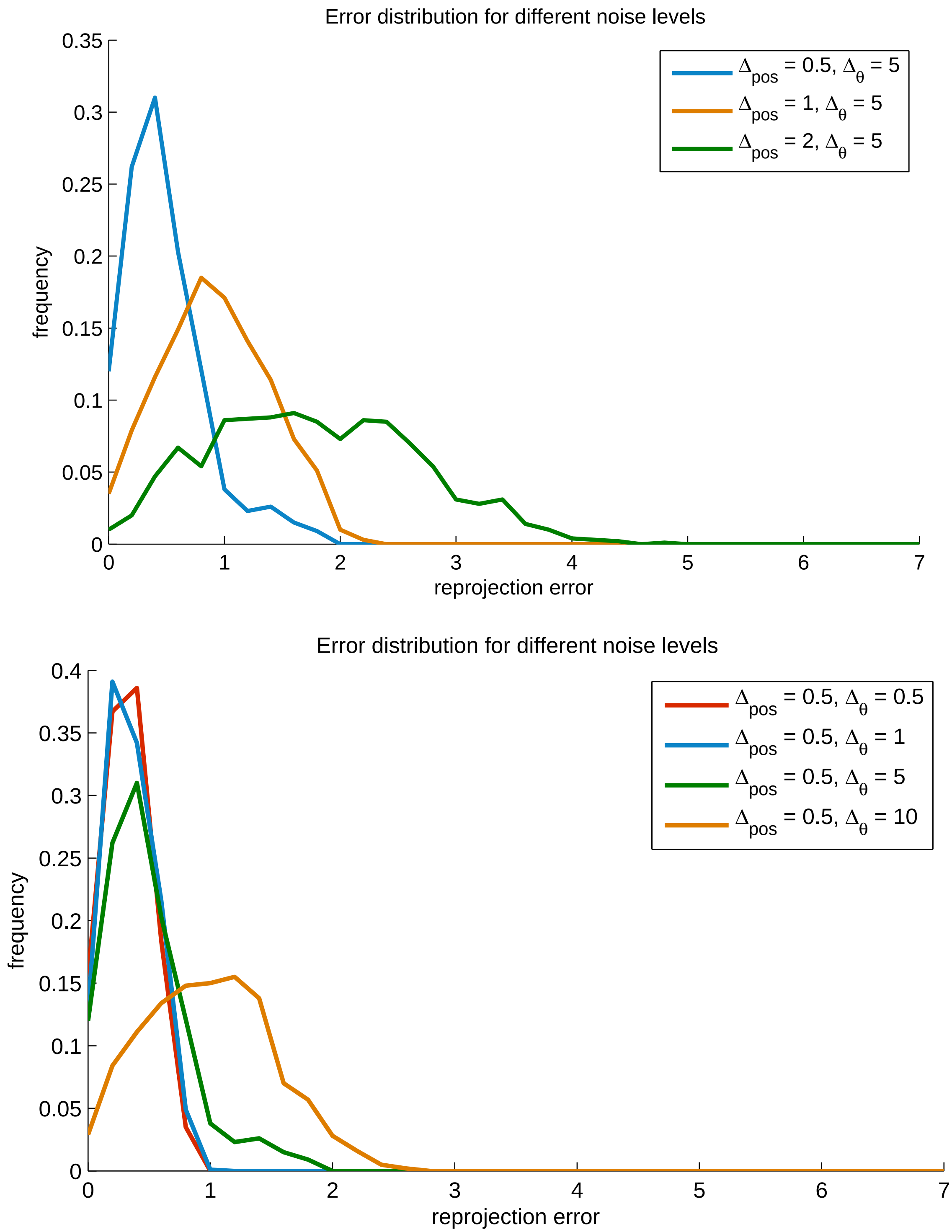

Figure 1: Distributions of reprojection error for synthetic data results **without bundle adjustment**, for (top) increasing levels of positional perturbation while keeping tangential orientation perturbation fixed; and (bottom) increasing levels of tangential orientation perturbation while keeping positional perturbation fixed. This is the same as in the paper, but split into two different plots for clarity.

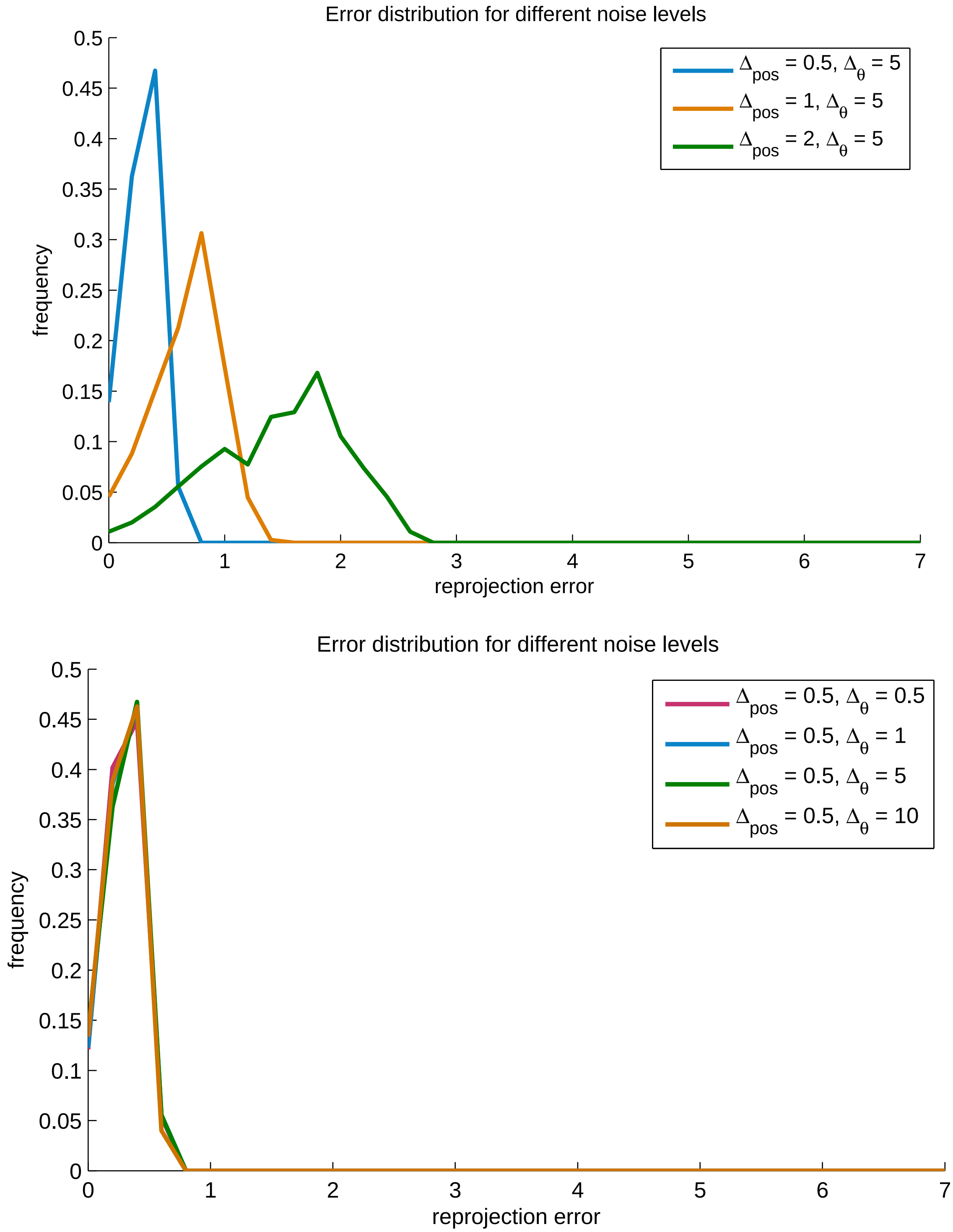

Figure 2: Distributions of reprojection error for synthetic data results **with bundle adjustment**, for (top) increasing levels of positional perturbation while keeping tangential orientation perturbation fixed; and (bottom) increasing levels of tangential orientation perturbation while keeping positional perturbation fixed.

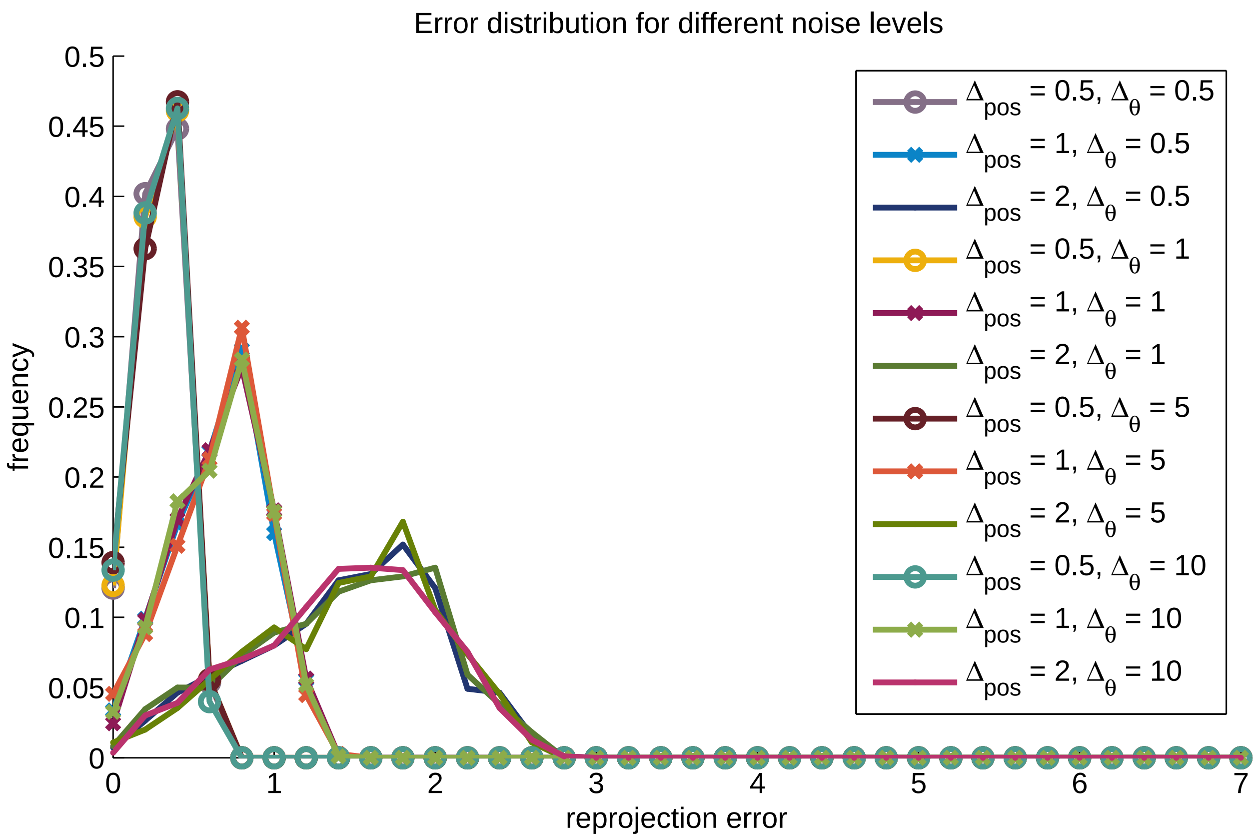

Figure 3: Full set of distributions of reprojection error for synthetic data results **with bundle adjustment**, for increasing levels of positional perturbation and tangential orientation perturbation. This is the same experiment as in Figure 2.

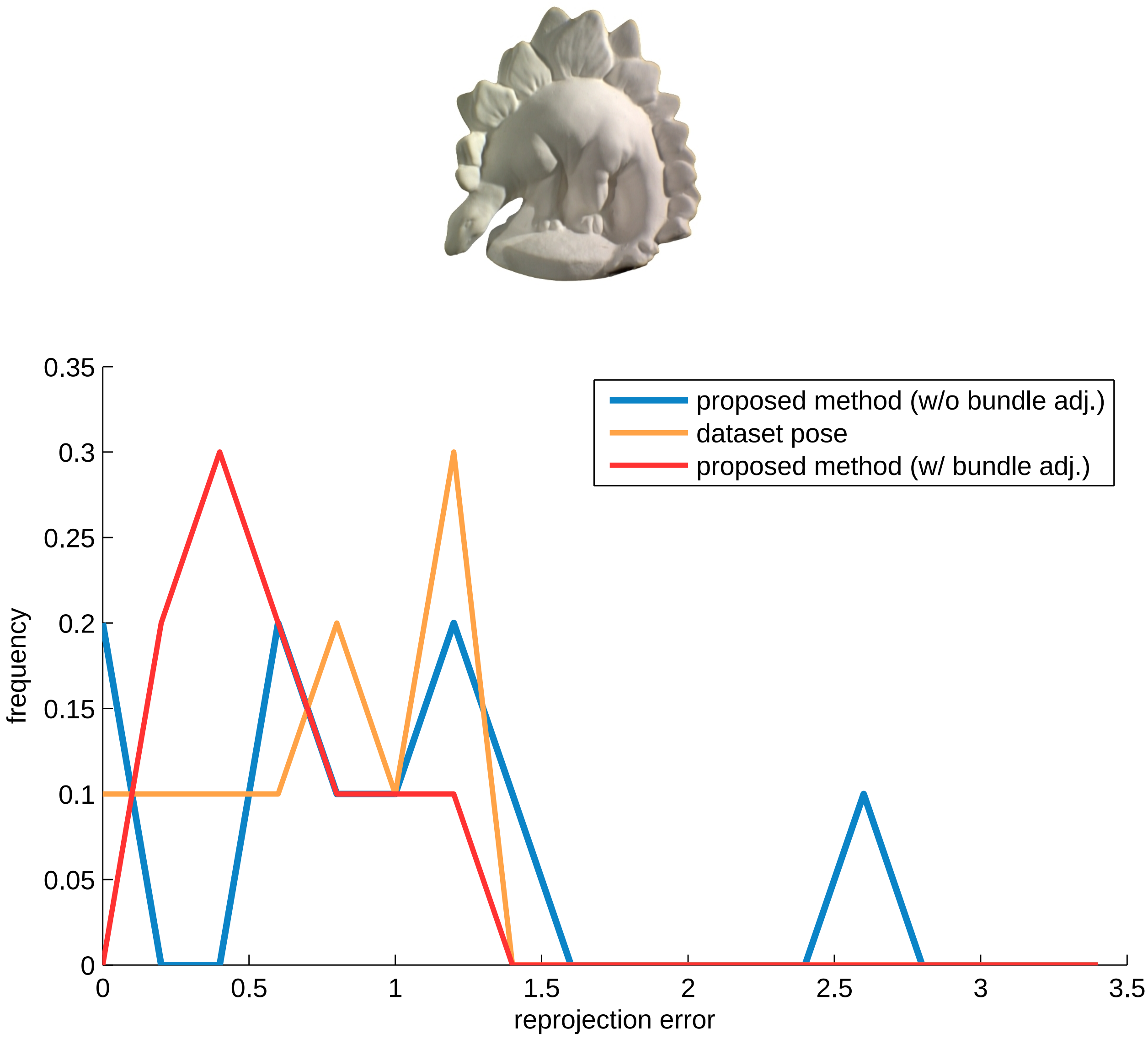

Figure 4: The reprojection error distributions for the standard Dino sequence from the Middlebury multiview stereo database [1], with a sample image shown at the top, using only two point-tangents selected within a RANSAC framework from 10 manual correspondences plus 50% outliers, before and after bundle adjustment. The average reprojection error for the proposed method are $1.03px$ and $0.66px$ before and after bundle adjustment, respectively, while the average error using the dataset camera is $0.88px$.

3 Detailed proof of Theorem 3.1

In the course of proving Theorem 3.1, we will *also* show that

$$\begin{aligned} Q(\rho_1,\rho_2) &= A^3(EH^2-FHK+GK^2)^2+AC^2(EJ^2-FJL+GL^2)^2 \\ &-2A^2C(EH^2-FHK+GK^2)(EJ^2-FJL+GL^2)+[-AB(EH^2-FHK+GK^2) \\ &+BC(EJ^2-FJL+GL^2)]\,[A(2EHJ-FHL-FJK+2GKL)-B(EJ^2-FJL+GL^2)] \\ &+C[A(2EHJ-FHL-FJK+2GKL)-B(EJ^2-FJL+GL^2)]^2=0 \end{aligned} \tag{1}$$

where the parameters A through L are defined as

$$\begin{cases} A = 1-2\boldsymbol{\gamma}_1^\top \boldsymbol{t}_1 B_1+\boldsymbol{\gamma}_1^\top\boldsymbol{\gamma}_1 B_1^2 \\ B = [2(\boldsymbol{\gamma}_1^\top \boldsymbol{t}_1)-2\boldsymbol{\gamma}_1^\top\boldsymbol{\gamma}_1 B_1]A_1 \\ C = (\boldsymbol{\gamma}_1^\top\boldsymbol{\gamma}_1)A_1^2-1 \\ E = 1-2\boldsymbol{\gamma}_2^\top \boldsymbol{t}_2 B_2+\boldsymbol{\gamma}_2^\top\boldsymbol{\gamma}_2 B_2^2 \\ F = [2(\boldsymbol{\gamma}_2^\top \boldsymbol{t}_2)-2\boldsymbol{\gamma}_2^\top\boldsymbol{\gamma}_2 B_2]A_2 \\ G = (\boldsymbol{\gamma}_2^\top\boldsymbol{\gamma}_2)A_2^2-1 \\ H = \boldsymbol{\gamma}_1^\top\boldsymbol{\gamma}_2 A_1A_2-(\boldsymbol{T}_1^w)^\top\boldsymbol{T}_2^w \\ J = [\boldsymbol{\gamma}_2^\top \boldsymbol{t}_1-\boldsymbol{\gamma}_1^\top\boldsymbol{\gamma}_2 B_1]A_2 \\ K = [\boldsymbol{\gamma}_1^\top \boldsymbol{t}_2-\boldsymbol{\gamma}_1^\top\boldsymbol{\gamma}_2 B_2]A_1 \\ L = \boldsymbol{t}_1^\top\boldsymbol{t}_2-\boldsymbol{\gamma}_2^\top\boldsymbol{t}_1 B_2-\boldsymbol{\gamma}_1^\top\boldsymbol{t}_2 B_1+\boldsymbol{\gamma}_1^\top\boldsymbol{\gamma}_2 B_1B_2, \end{cases} \tag{2}$$

where

$$\begin{cases} A_1 = \dfrac{(\boldsymbol{\Gamma}_1^w-\boldsymbol{\Gamma}_2^w)^\top\boldsymbol{T}_1^w}{(\rho_1\boldsymbol{\gamma}_1-\rho_2\boldsymbol{\gamma}_2)^\top\boldsymbol{\gamma}_1} \\ A_2 = \dfrac{(\boldsymbol{\Gamma}_1^w-\boldsymbol{\Gamma}_2^w)^\top\boldsymbol{T}_2^w}{(\rho_1\boldsymbol{\gamma}_1-\rho_2\boldsymbol{\gamma}_2)^\top\boldsymbol{\gamma}_2} \end{cases} \qquad \begin{cases} B_1 = \dfrac{(\rho_1\boldsymbol{\gamma}_1-\rho_2\boldsymbol{\gamma}_2)^\top\boldsymbol{t}_1}{(\rho_1\boldsymbol{\gamma}_1-\rho_2\boldsymbol{\gamma}_2)^\top\boldsymbol{\gamma}_1} \\ B_2 = \dfrac{(\rho_1\boldsymbol{\gamma}_1-\rho_2\boldsymbol{\gamma}_2)^\top\boldsymbol{t}_2}{(\rho_1\boldsymbol{\gamma}_1-\rho_2\boldsymbol{\gamma}_2)^\top\boldsymbol{\gamma}_2}, \end{cases} \tag{3}$$

and where

$$\begin{cases} \rho_1\dfrac{g_1}{G_1} = -\dfrac{A(EH^2-FHK+GK^2)-C(EJ^2-FJL+GL^2)}{A(2EHJ-FHL-FJK+2GKL)-B(EJ^2-FJL+GL^2)}. \\ \rho_2\dfrac{g_2}{G_2} = -\dfrac{E(AH^2-BHJ+CJ^2)-G(AK^2-BKL+CL^2)}{E(2AHK-BHL-BKJ+2CJL)-F(AK^2-BKL+CL^2)}, \end{cases} \tag{4}$$

and

$$\begin{cases} \dfrac{\rho_1'}{G_1} = A_1-B_1\rho_1\dfrac{g_1}{G_1} \\ \dfrac{\rho_2'}{G_2} = A_2-B_2\rho_2\dfrac{g_2}{G_2}. \end{cases} \tag{5}$$

Proof. (*Of Theorem 3.1 and the above statements*) An image point $\boldsymbol{\gamma}$ is related to the underlying space point $\boldsymbol{\Gamma}$ through $\boldsymbol{\Gamma}=\rho\boldsymbol{\gamma}$, where ρ is depth. A space point $\boldsymbol{\Gamma}$ in local coordinates is related to $\boldsymbol{\Gamma}^w$ in the world coordinates by a rotation matrix $\mathcal{R}$ and translation $\mathcal{T}$ through $\boldsymbol{\Gamma}=\mathcal{R}\boldsymbol{\Gamma}^w+\mathcal{T}$. Equating these at each of the two points gives

$$\begin{cases} \rho_1\boldsymbol{\gamma}_1 = \mathcal{R}\boldsymbol{\Gamma}_1^w+\mathcal{T} \\ \rho_2\boldsymbol{\gamma}_2 = \mathcal{R}\boldsymbol{\Gamma}_2^w+\mathcal{T}, \end{cases} \tag{6}$$

where ρ_1 and ρ_2 are the depth at image points $\boldsymbol{\gamma}_1$ and $\boldsymbol{\gamma}_2$, respectively. By differentiating with respect to the parameters of γ_1 and $\boldsymbol{\gamma}_2$ we have:

$$\begin{cases} \rho_1 g_1\boldsymbol{t}_1+\rho_1'\gamma_1 = \mathcal{R}G_1\boldsymbol{T}_1^w \\ \rho_2 g_2\boldsymbol{t}_2+\rho_2'\gamma_2 = \mathcal{R}G_2\boldsymbol{T}_2^w, \end{cases} \tag{7}$$

where ρ_1 and ρ_2 are depth derivatives with respect to the curve parameter, g_1 and g_2 are speeds of parametrization of $\boldsymbol{\gamma}_1$ and $\boldsymbol{\gamma}_2$, respectively, and G_1 and G_2 are the speeds of parametrization of the space curves $\mathbf{\Gamma}_1$ and $\mathbf{\Gamma}_2$, respectively. The vector Equations 6 and 7 represent 3 scalar equations for each point, so that there are 12 equations in all. The parametrization speeds g_1 and g_2 are arbitrary and can be set to 1 uniformly, but we keep them in general form. The given quantities are $\boldsymbol{\gamma}$, $\boldsymbol{t}$, and $\mathbf{\Gamma}^w$, $\boldsymbol{T}^w$ at each point. The unknowns are $\mathcal{R}$, $\mathcal{T}$ (6 unknowns), ρ, ρ' (4 unknowns), and the two speeds of the curve Γ at the two points, 12 unknowns in all. Therefore, in principle, two points should provide enough constraints to solve the problem.

First, $\mathcal{T}$ is eliminated by subtracting the two Equations (6)

$$\rho_1\boldsymbol{\gamma}_1 - \rho_2\boldsymbol{\gamma}_2 = \mathcal{R}(\mathbf{\Gamma}_1^w - \mathbf{\Gamma}_2^w), \tag{8}$$

which together with Equation 7 gives a system of equations

$$\begin{cases} \rho_1\boldsymbol{\gamma}_1 - \rho_2\boldsymbol{\gamma}_2 = \mathcal{R}(\mathbf{\Gamma}_1^w - \mathbf{\Gamma}_2^w) & (9)\\ \rho_1\dfrac{g_1}{G_1}\boldsymbol{t}_1 + \dfrac{\rho_1'}{G_1}\boldsymbol{\gamma}_1 = \mathcal{R}\boldsymbol{T}_1^w & (10)\\ \rho_2\dfrac{g_2}{G_2}\boldsymbol{t}_2 + \dfrac{\rho_2'}{G_2}\boldsymbol{\gamma}_2 = \mathcal{R}\boldsymbol{T}_2^w. & (11)\end{cases}$$

At this stage, the unknowns are ρ_1, ρ_2, $\frac{\rho_1'}{G_1}$, $\frac{\rho_2'}{G_2}$, $\rho_1\frac{g_1}{G_1}$, $\rho_2\frac{g_2}{G_2}$, and $\mathcal{R}$, nine numbers in all, which can potentially be solved through the three vector equations (nine scalar equations) in (9)–(11). The number of unknowns can be reduced by eliminating $\mathcal{R}$ in a second step. The matrix $\mathcal{R}$ rotates three known vectors, $(\mathbf{\Gamma}_1^w - \mathbf{\Gamma}_2^w)$, $\boldsymbol{T}_1^w$, and $\boldsymbol{T}_2^w$ to the three unknown vectors on the left side of these equations, requiring a preservation of vector lengths and mutual angles. The length and relative angles are obtained from the known dot products, which do not involve $\mathcal{R}$ at all. This provides six equations for the six unknowns $\{\rho_1, \rho_2, \frac{g_1}{G_1}, \frac{g_2}{G_2}, \frac{\rho_1'}{G_1}, \frac{\rho_2'}{G_2}\}$. Alternatively, we write these three equations in matrix form composed from the three vector equations (9)–(11), *i.e.*,

$$\left[\rho_1\boldsymbol{\gamma}_1 - \rho_2\boldsymbol{\gamma}_2 \quad \rho\tfrac{g_1}{G_1}\boldsymbol{t}_1 + \tfrac{\rho_1'}{G_1}\boldsymbol{\gamma}_1 \quad \rho_2\tfrac{g_2}{G_2}\boldsymbol{t}_2 + \tfrac{\rho_2'}{G_2}\boldsymbol{\gamma}_2\right] = \mathcal{R}\left[(\mathbf{\Gamma}_1^w - \mathbf{\Gamma}_2^w) \quad \boldsymbol{T}_1^w \quad \boldsymbol{T}_2^w\right] \tag{12}$$

This is a system of six equations. Note that a clear geometric condition for the problem to have a solution is that the vectors $\{(\mathbf{\Gamma}_1^w - \mathbf{\Gamma}_2^w),\ \boldsymbol{T}_1^w,\ \boldsymbol{T}_2^w\}$ be non-coplanar. Using product of the left hand matrix with its transpose, and using $\mathcal{R}^\top\mathcal{R} = I$, gives

$$\begin{cases} (\rho_1\boldsymbol{\gamma}_1 - \rho_2\boldsymbol{\gamma}_2)^\top(\rho_1\boldsymbol{\gamma}_1 - \rho_2\boldsymbol{\gamma}_2) = (\mathbf{\Gamma}_1^w - \mathbf{\Gamma}_2^w)^\top(\mathbf{\Gamma}_1^w - \mathbf{\Gamma}_2^w)\\ (\rho_1\boldsymbol{\gamma}_1 - \rho_2\boldsymbol{\gamma}_2)^\top(\rho_1\dfrac{g_1}{G_1}\boldsymbol{t}_1 + \dfrac{\rho_1'}{G_1}\boldsymbol{\gamma}_1) = (\mathbf{\Gamma}_1^w - \mathbf{\Gamma}_2^w)^\top\boldsymbol{T}_1^w\\ (\rho_1\boldsymbol{\gamma}_1 - \rho_2\boldsymbol{\gamma}_2)^\top(\rho_2\dfrac{g_2}{G_2}\boldsymbol{t}_2 + \dfrac{\rho_2'}{G_2}\boldsymbol{\gamma}_1) = (\mathbf{\Gamma}_2^w - \mathbf{\Gamma}_2^w)^\top\boldsymbol{T}_2^w\\ (\rho_1\dfrac{g_1}{G_1}\boldsymbol{t}_1 + \dfrac{\rho_1'}{G_1}\boldsymbol{\gamma}_1)^\top(\rho_1\dfrac{g_1}{G_1}\boldsymbol{t}_1 + \dfrac{\rho_1'}{G_1}\boldsymbol{\gamma}_1) = 1\\ (\rho_2\dfrac{g_2}{G_2}\boldsymbol{t}_2 + \dfrac{\rho_2'}{G_2}\boldsymbol{\gamma}_2)^\top(\rho_2\dfrac{g_2}{G_2}\boldsymbol{t}_2 + \dfrac{\rho_2'}{G_2}\boldsymbol{\gamma}_2) = 1\\ (\rho_1\dfrac{g_1}{G_1}\boldsymbol{t}_1 + \dfrac{\rho_1'}{G_1}\boldsymbol{\gamma}_1)^\top(\rho_2\dfrac{g_2}{G_2}\boldsymbol{t}_2 + \dfrac{\rho_2'}{G_2}\boldsymbol{\gamma}_2) = (\boldsymbol{T}_1^w)^\top\boldsymbol{T}_2^w. \end{cases} \tag{13}$$

The first equation is a quadratic in ρ_1 and ρ_2

$$\boldsymbol{\gamma}_1^\top\boldsymbol{\gamma}_1\,\rho_1^2 - 2\boldsymbol{\gamma}_1^\top\boldsymbol{\gamma}_2\,\rho_1\rho_2 + \boldsymbol{\gamma}_2^\top\boldsymbol{\gamma}_2\,\rho_2^2 = (\mathbf{\Gamma}_1^w - \mathbf{\Gamma}_2^w)^\top(\mathbf{\Gamma}_1^w - \mathbf{\Gamma}_2^w), \tag{14}$$

which as a conic in the ρ_1–ρ_2 plane with negative discriminant

$$(\boldsymbol{\gamma}_1\cdot\boldsymbol{\gamma}_2)^2 - (\boldsymbol{\gamma}_1\cdot\boldsymbol{\gamma}_1)(\boldsymbol{\gamma}_2\cdot\boldsymbol{\gamma}_2) = -\|\boldsymbol{\gamma}_1\times\boldsymbol{\gamma}_2\|^2 < 0 \tag{15}$$

is an ellipse. The ellipse is centered at the origin so we can check that it has real points by solving for ρ_1 when $\rho_2 = 0$, giving $\rho_1^2\|\boldsymbol{\gamma}_1\|^2 = \|\boldsymbol{\Gamma}_1^w - \boldsymbol{\Gamma}_2^w\|^2$, or real roots $\rho_1 = \pm\frac{\|\boldsymbol{\Gamma}_1^w - \boldsymbol{\Gamma}_2^w\|}{\|\boldsymbol{\gamma}_1\|}$.

The remaining five equations involve the additional unknowns $\{\rho_1\frac{g_1}{G_1}, \rho_2\frac{g_2}{G_2}, \frac{\rho_1'}{G_1}, \frac{\rho_2'}{G_2}\}$. The latter appear in a linear form in the second and third equations, and in quadratic form in the last three equations. Thus, the terms $\frac{\rho_1'}{G_1}$ and $\frac{\rho_2'}{G_2}$ can be isolated from the second and third equations and then used in the last three equations

$$\begin{cases} [(\rho_1\boldsymbol{\gamma}_1 - \rho_2\boldsymbol{\gamma}_2)^\top\boldsymbol{\gamma}_1]\dfrac{\rho_1'}{G_1} = (\boldsymbol{\Gamma}_1^w - \boldsymbol{\Gamma}_2^w)^\top\boldsymbol{T}_1^w - [(\rho_1\boldsymbol{\gamma}_1 - \rho_2\boldsymbol{\gamma}_2)^\top\boldsymbol{t}_1]\rho_1\dfrac{g_1}{G_1} \\ [(\rho_1\boldsymbol{\gamma}_1 - \rho_2\boldsymbol{\gamma}_2)^\top\boldsymbol{\gamma}_2]\dfrac{\rho_2'}{G_2} = (\boldsymbol{\Gamma}_1^w - \boldsymbol{\Gamma}_2^w)^\top\boldsymbol{T}_2^w - [(\rho_1\boldsymbol{\gamma}_1 - \rho_2\boldsymbol{\gamma}_2)^\top\boldsymbol{t}_2]\rho_2\dfrac{g_2}{G_2}, \end{cases} \tag{16}$$

or

$$\begin{cases} \dfrac{\rho_1'}{G_1} = \dfrac{(\boldsymbol{\Gamma}_1^w - \boldsymbol{\Gamma}_2^w)^\top\boldsymbol{T}_1^w}{(\rho_1\boldsymbol{\gamma}_1 - \rho_2\boldsymbol{\gamma}_2)^\top\boldsymbol{\gamma}_1} - \left[\dfrac{(\rho_1\boldsymbol{\gamma}_1 - \rho_2\boldsymbol{\gamma}_2)^\top\boldsymbol{t}_1}{(\rho_1\boldsymbol{\gamma}_1 - \rho_2\boldsymbol{\gamma}_2)^\top\boldsymbol{\gamma}_1}\right]\rho_1\dfrac{g_1}{G_1} \quad = A_1 - B_1\rho_1\dfrac{g_1}{G_1} \\ \dfrac{\rho_2'}{G_2} = \dfrac{(\boldsymbol{\Gamma}_1^w - \boldsymbol{\Gamma}_2^w)^\top\boldsymbol{T}_2^w}{(\rho_1\boldsymbol{\gamma}_1 - \rho_2\boldsymbol{\gamma}_2)^\top\boldsymbol{\gamma}_2} - \left[\dfrac{(\rho_1\boldsymbol{\gamma}_1 - \rho_2\boldsymbol{\gamma}_2)^\top\boldsymbol{t}_2}{(\rho_1\boldsymbol{\gamma}_1 - \rho_2\boldsymbol{\gamma}_2)^\top\boldsymbol{\gamma}_2}\right]\rho_2\dfrac{g_2}{G_2} \quad = A_2 - B_2\rho_2\dfrac{g_2}{G_2}, \end{cases} \tag{17}$$

noting that A_1, A_2, B_1, and B_2 depend on only two of the unknowns ρ_1 and ρ_2. The last three equations in (13) can be expanded as

$$\begin{cases} \left(\rho_1\dfrac{g_1}{G_1}\right)^2 + 2(\boldsymbol{\gamma}_1^\top\boldsymbol{t}_1)\left(\rho_1\dfrac{g_1}{G_1}\right)\left(\dfrac{\rho_1'}{G_1}\right) + (\boldsymbol{\gamma}_1^\top\boldsymbol{\gamma}_1)\left(\dfrac{\rho_1'}{G_1}\right)^2 = 1 \\ \left(\rho_2\dfrac{g_2}{G_2}\right)^2 + 2(\boldsymbol{\gamma}_2^\top\boldsymbol{t}_2)\left(\rho_2\dfrac{g_2}{G_2}\right)\left(\dfrac{\rho_2'}{G_2}\right) + (\boldsymbol{\gamma}_2^\top\boldsymbol{\gamma}_2)\left(\dfrac{\rho_2'}{G_2}\right)^2 = 1 \\ (\boldsymbol{t}_1^\top\boldsymbol{t}_2)\left(\rho_1\dfrac{g_1}{G_1}\right)\left(\rho_2\dfrac{g_2}{G_2}\right) + (\boldsymbol{\gamma}_2^\top\boldsymbol{t}_1)\left(\rho_1\dfrac{g_1}{G_1}\right)\left(\dfrac{\rho_2'}{G_2}\right) + (\boldsymbol{\gamma}_1^\top\boldsymbol{t}_2)\left(\rho_2\dfrac{g_2}{G_2}\right)\left(\dfrac{\rho_1'}{G_1}\right) + \\ \qquad (\boldsymbol{\gamma}_1^\top\boldsymbol{\gamma}_2)\left(\dfrac{\rho_1'}{G_1}\right)\left(\dfrac{\rho_2'}{G_2}\right) = (\boldsymbol{T}_1^w)^\top\boldsymbol{T}_2^w. \end{cases}$$

Substituting $\frac{\rho_1'}{G_1}$ and $\frac{\rho_2'}{G_2}$ from Equations 17 gives

$$\begin{cases} \left(\rho_1\dfrac{g_1}{G_1}\right)^2 + 2(\boldsymbol{\gamma}_1^\top\boldsymbol{t}_1)\left(\rho_1\dfrac{g_1}{G_1}\right)\left(A_1 - B_1\left(\rho_1\dfrac{g_1}{G_1}\right)\right) + (\boldsymbol{\gamma}_1^\top\boldsymbol{\gamma}_1)\left(A_1 - B_1\left(\rho_1\dfrac{g_1}{G_1}\right)\right)^2 = 1 \\ \left(\rho_2\dfrac{g_2}{G_2}\right)^2 + 2(\boldsymbol{\gamma}_2^\top\boldsymbol{t}_2)\left(\rho_2\dfrac{g_2}{G_2}\right)\left(A_2 - B_2\left(\rho_2\dfrac{g_2}{G_2}\right)\right) + (\boldsymbol{\gamma}_2^\top\boldsymbol{\gamma}_2)\left(A_2 - B_2\left(\rho_2\dfrac{g_2}{G_2}\right)\right)^2 = 1 \\ (\boldsymbol{t}_1^\top\boldsymbol{t}_2)\left(\rho_1\dfrac{g_1}{G_1}\right)\left(\rho_2\dfrac{g_2}{G_2}\right) + (\boldsymbol{\gamma}_2^\top\boldsymbol{t}_1)\left(\rho_1\dfrac{g_1}{G_1}\right)\left(A_2 - B_2\left(\rho_2\dfrac{g_2}{G_2}\right)\right) + \\ (\boldsymbol{\gamma}_1^\top\boldsymbol{t}_2)\left(\rho_2\dfrac{g_2}{G_2}\right)\left(A_1 - B_1\left(\rho_1\dfrac{g_1}{G_1}\right)\right) + (\boldsymbol{\gamma}_1^\top\boldsymbol{\gamma}_2)\left(A_1 - B_1\left(\rho_1\dfrac{g_1}{G_1}\right)\right)\left(A_2 - B_2\left(\rho_2\dfrac{g_2}{G_2}\right)\right) \\ = (\boldsymbol{T}_1^w)^\top\boldsymbol{T}_2^w. \end{cases}$$

These three equations can be written in summary form using $x_1 = \rho_1\frac{g_1}{G_1}$ and $x_2 = \rho_2\frac{g_2}{G_2}$,

$$Ax_1^2 + Bx_1 + C = 0 \tag{18}$$

$$Ex_2^2 + Fx_2 + G = 0 \tag{19}$$

$$H + Jx_1 + Kx_2 + Lx_1x_2 = 0, \tag{20}$$

and where A through L are only functions of the two unknowns ρ_1 and ρ_2. Thus, the three Equations 18–20 after solving for x_1 and x_2 express a relationship between ρ_1 and ρ_2, which together with Equation 14 can lead to a solution for ρ_1 and ρ_2.

Equation 20, with given values for ρ_1 and ρ_2, represents a rectangular hyperbola in the x_1–x_2 plane, as illustrated in the paper, and each of the Equations 18 and 19 represents a pair of (real) lines in the same plane, parallel respectively to the x_2 and x_1 axes. In general there will not be more than one intersection between the aforementioned curves.

Specifically, the variables x_1 and x_2 can be solved by rewriting Equation 20 as

$$(H + Jx_1) + (K + Lx_1)x_2 = 0, \tag{21}$$

giving

$$x_2 = -\frac{H + Jx_1}{K + Lx_1}. \tag{22}$$

Using this expression in Equation 19 gives

$$E\frac{(H + Jx_1)^2}{(K + Lx_1)^2} - F\frac{H + Jx_1}{K + Lx_1} + G = 0, \tag{23}$$

or

$$E(H + Jx_1)^2 - F(H + Jx_1)(K + Lx_1) + G(K + Lx_1)^2 = 0. \tag{24}$$

Reorganizing as a quadratic in x_1, this solves for x_1 which together with Equation 18 gives a constraint on the parameters depending on ρ_1 and ρ_2,

$$\begin{cases} (EJ^2 - FJL + GL^2)x_1^2 + (2EHJ - FHL - FJK + 2GKL)x_1 & (25) \\ \quad +(EH^2 - FHK + GK^2) = 0 & \\ \qquad Ax_1^2 + Bx_1 + C = 0. & (26) \end{cases}$$

The quadratic term is eliminated by multiplying the first equation by A and the second equation by $(EJ^2 - FJL + GL^2)$ and subtracting, giving

$$\begin{aligned} &[A(2EHJ - FHL - FJK + 2GKL) - B(EJ^2 - FJL + GL^2)]x_1 + \\ &\qquad [A(EH^2 - FHK + GK^2) - C(EJ^2 - FJL + GL^2)] = 0, \end{aligned} \tag{27}$$

so that

$$x_1 = -\frac{A(EH^2 - FHK + GK^2) - C(EJ^2 - FJL + GL^2)}{A(2EHJ - FHL - FJK + 2GKL) - B(EJ^2 - FJL + GL^2)}. \tag{28}$$

Substituting back into Equation 26 gives

$$\begin{aligned} &A\left[\frac{A(EH^2 - FHK + GK^2) - C(EJ^2 - FJL + GL^2)}{A(2EHJ - FHL - FJK + 2GKL) - B(EJ^2 - FJL + GL^2)}\right]^2 + \\ &-B\frac{A(EH^2 - FHK + GK^2) - C(EJ^2 - FJL + GL^2)}{A(2EHJ - FHL - FJK + 2GKL) - B(EJ^2 - FJL + GL^2)} + C = 0, \end{aligned} \tag{29}$$

or

$$\begin{aligned} &A^3(EH^2 - FHK + GK^2)^2 + AC^2(EJ^2 - FJL + GL^2)^2 \\ &- 2A^2C(EH^2 - FHK + GK^2)(EJ^2 - FJL + GL^2) + [-AB(EH^2 - FHK + GK^2) \\ &+ BC(EJ^2 - FJL + GL^2)]\,[A(2EHJ - FHL - FJK + 2GKL) - B(EJ^2 - FJL + GL^2)] \\ &+ C[A(2EHJ - FHL - FJK + 2GKL) - B(EJ^2 - FJL + GL^2)]^2 = 0 \end{aligned} \tag{30}$$

The equation, after expressions for $A, B, \ldots, L$ are substituted in, can be divided by $\rho_1^4\rho_2^4$, giving an 8^{th} order polynomial equation in ρ_1 and ρ_2, *i.e.*, $Q(\rho_1, \rho_2) = 0$. This equation together with Equation 14 represents a system of two equations in two unknowns

$$\begin{cases} \boldsymbol{\gamma}_1^\top \boldsymbol{\gamma}_1\, \rho_1^2 - 2\boldsymbol{\gamma}_1^\top \boldsymbol{\gamma}_2\, \rho_1\rho_2 + \boldsymbol{\gamma}_2^\top \boldsymbol{\gamma}_2\, \rho_2^2 = (\boldsymbol{\Gamma}_1^w - \boldsymbol{\Gamma}_2^w)^\top(\boldsymbol{\Gamma}_1^w - \boldsymbol{\Gamma}_2^w), \\ Q(\rho_1, \rho_2) = 0, \end{cases} \tag{31}$$

and gives a number of solutions for ρ_1, and ρ_2 which in turn solve for the unknowns $\rho_1 \frac{g_1}{G_1}$, $\rho_2 \frac{g_2}{G_2}$, $\frac{\rho_1'}{G_1}$, and $\frac{\rho_2}{G_2}$. Once these unknowns are solved for, the rotation $\mathcal{R}$ can be obtained from the matrix equation (12). The translation $\mathcal{T}$ is then solved from Equations 6 as

$$\mathcal{T} = \rho_1 \boldsymbol{\gamma}_1 - \mathcal{R}\boldsymbol{\Gamma}_1^w. \tag{32}$$

□

4 Details in the Proof of Proposition 3.2

The parametrization we have assumed in the space curve projects $\boldsymbol{T}$ to the same half plane as $\boldsymbol{t}$ in each view so that $\boldsymbol{T}$ and $\boldsymbol{t}$ need to point in the same direction, *i.e.*, $\boldsymbol{T} \cdot \boldsymbol{t} > 0$, or from Equations 10 and 11, $\frac{g_1}{G_1} > 0$ and $\frac{g_2}{G_2} > 0$.

5 Details in the Proof of Proposition 4.1

The parameters α, β, and θ for the ellipse in Equation 14 can be found by substitution of ρ_1 and ρ_2 in the parametric form (given in the paper) into Equation 14. Specifically, writing

$$\begin{aligned}
&\frac{\boldsymbol{\gamma}_1^\top \boldsymbol{\gamma}_1}{(1+t^2)^2}[4\alpha^2 t^2 \cos^2\theta + \beta^2(1-t^2)^2 \sin^2\theta + 4\alpha\beta t(1-t^2)\sin\theta\cos\theta] + \\
&-\frac{2\boldsymbol{\gamma}_1^\top \boldsymbol{\gamma}_2}{(1+t^2)^2}[-4\alpha^2 t^2 \sin\theta\cos\theta + 2\alpha\beta t(1-t^2)\cos^2\theta - 2\alpha\beta t(1-t^2)\sin^2\theta] + \beta^2(1-t^2)^2\sin\theta\cos\theta \\
&\frac{-2\boldsymbol{\gamma}_2^\top \boldsymbol{\gamma}_2}{(1+t^2)^2}[4\alpha^2 t^2 \sin^2\theta + \beta^2(1-t^2)^2\cos^2\theta - 4\alpha\beta t(1-t^2)\sin\theta\cos\theta] = \|\boldsymbol{\Gamma}_1^w - \boldsymbol{\Gamma}_2^w\|^2.
\end{aligned} \tag{33}$$

Simplifying the equation as

$$\begin{aligned}
&[(\boldsymbol{\gamma}_1^\top \boldsymbol{\gamma}_1)4\alpha^2 t^2 - (\boldsymbol{\gamma}_1^\top \boldsymbol{\gamma}_2)4\alpha\beta t(1-t^2) + (\boldsymbol{\gamma}_2^\top \boldsymbol{\gamma}_2)\beta^2(1-t^2)^2]\cos^2\theta + \\
&[(\boldsymbol{\gamma}_1^\top \boldsymbol{\gamma}_1)\beta^2(1-t^2)^2 + (\boldsymbol{\gamma}_1^\top \boldsymbol{\gamma}_2)4\alpha\beta t(1-t^2)(\boldsymbol{\gamma}_2^\top \boldsymbol{\gamma}_2)4\alpha^2 t^2]\sin^2\theta + \\
&[(\boldsymbol{\gamma}_1^\top \boldsymbol{\gamma}_1)4\alpha\beta t(1-t^2) + (\boldsymbol{\gamma}_1^\top \boldsymbol{\gamma}_2 8\alpha^2 t^2 - (\boldsymbol{\gamma}_1^\top \boldsymbol{\gamma}_2)2\beta^2(1-t^2)^2 - (\boldsymbol{\gamma}_2^\top \boldsymbol{\gamma}_2)4\alpha\beta t(1-t^2)]\sin\theta\cos\theta \\
&= (1+t^2)^2\|\boldsymbol{\Gamma}_1^w - \boldsymbol{\Gamma}_2^w\|^2
\end{aligned} \tag{34}$$

and using simple trigonometric identities $\cos^2\theta = \frac{1+\cos(2\theta)}{2}$ and $\sin^2\theta = \frac{1-\sin(2\theta)}{2}$, $\cos^2\theta - \sin^2\theta = \cos(2\theta)$ and $\sin(2\theta) = 2\sin\theta\cos\theta$, this equation can be better simplified to

$$\begin{aligned}
&[(\boldsymbol{\gamma}_1^\top \boldsymbol{\gamma}_1)4\alpha^2 t^2 - (\boldsymbol{\gamma}_1^\top \boldsymbol{\gamma}_2)4\alpha\beta t(1-t^2) + (\boldsymbol{\gamma}_2^\top \boldsymbol{\gamma}_2)\beta^2(1-t^2)^2](1+\cos(2\theta)) + \\
&[(\boldsymbol{\gamma}_1^\top \boldsymbol{\gamma}_1)\beta^2(1-t^2)^2 + (\boldsymbol{\gamma}_1^\top \boldsymbol{\gamma}_2)4\alpha\beta t(1-t^2) + (\boldsymbol{\gamma}_2^\top \boldsymbol{\gamma}_2)4\alpha^2 t^2](1-\cos(2\theta)) + \\
&[(\boldsymbol{\gamma}_1^\top \boldsymbol{\gamma}_1)4\alpha\beta t(1-t^2) + (\boldsymbol{\gamma}_1^\top \boldsymbol{\gamma}_2)8\alpha^2 t^2 - (\boldsymbol{\gamma}_1^\top \boldsymbol{\gamma}_2)2\beta^2(1-t^2)^2 - (\boldsymbol{\gamma}_2^\top \boldsymbol{\gamma}_2)4\alpha\beta t(1-t^2)]\sin(2\theta) \\
&= 2(1+t^2)^2\|\boldsymbol{\Gamma}_1^w - \boldsymbol{\Gamma}_2^w\|^2.
\end{aligned} \tag{35}$$

which is an equation only involving the unknown θ,

$$\begin{aligned}
&(\boldsymbol{\gamma}_1^\top \boldsymbol{\gamma}_1 + \boldsymbol{\gamma}_2^\top \boldsymbol{\gamma}_2)[4\alpha^2 t^2 + \beta^2(1-t^2)] + \\
&[(\boldsymbol{\gamma}_1^\top \boldsymbol{\gamma}_1 - \boldsymbol{\gamma}_2^\top \boldsymbol{\gamma}_2)[4\alpha^2 t^2 - \beta^2(1-t^2)^2] - (\boldsymbol{\gamma}_1^\top \boldsymbol{\gamma}_2)8\alpha\beta t(1-t^2)]\cos(2\theta) \\
&[(\boldsymbol{\gamma}_1^\top \boldsymbol{\gamma}_1 - \boldsymbol{\gamma}_2^\top \boldsymbol{\gamma}_2)4\alpha\beta t(1-t^2) + 2\boldsymbol{\gamma}_1^\top \boldsymbol{\gamma}_2[4\alpha^2 t^2 - \beta^2(1-t^2)^2]]\sin(2\theta) \\
&= 2(1+t^2)^2\|\boldsymbol{\Gamma}_1^w - \boldsymbol{\Gamma}_2^w\|^2.
\end{aligned} \tag{36}$$

This equation holds for all values of t. For $t = 0$,

$$(\boldsymbol{\gamma}_1^\top \boldsymbol{\gamma}_1 + \boldsymbol{\gamma}_2^\top \boldsymbol{\gamma}_2)\beta^2 - (\boldsymbol{\gamma}_1^\top \boldsymbol{\gamma}_2 - \boldsymbol{\gamma}_2^\top \boldsymbol{\gamma}_2)\beta^2\cos(2\theta) - 2\boldsymbol{\gamma}_1^\top \boldsymbol{\gamma}_2\beta^2\sin(2\theta) = 2\|\boldsymbol{\Gamma}_1^w - \boldsymbol{\Gamma}_2^w\|, \tag{37}$$

giving

$$\beta^2 = \frac{2\|\mathbf{\Gamma}_1^w - \mathbf{\Gamma}_2^w\|^2}{(\boldsymbol{\gamma}_1^\top \boldsymbol{\gamma}_1 + \boldsymbol{\gamma}_2^\top \boldsymbol{\gamma}_2) - (\boldsymbol{\gamma}_1^\top \boldsymbol{\gamma}_1 - \boldsymbol{\gamma}_2^\top \boldsymbol{\gamma}_2)\cos(2\theta) - 2\boldsymbol{\gamma}_1^\top \boldsymbol{\gamma}_2 \sin(2\theta)}. \tag{38}$$

Similarly, at $t = 1$,

$$(\boldsymbol{\gamma}_1^\top \boldsymbol{\gamma}_1 + \boldsymbol{\gamma}_2^\top \boldsymbol{\gamma}_2)4\alpha^2 + (\boldsymbol{\gamma}_1^\top \boldsymbol{\gamma}_1 - \boldsymbol{\gamma}_2^\top \boldsymbol{\gamma}_2)4\alpha^2 \cos(2\theta) + 2\boldsymbol{\gamma}_1^\top \boldsymbol{\gamma}_2 4\alpha^2 \sin(2\theta) = 8\|\mathbf{\Gamma}_1^w - \mathbf{\Gamma}_2^w\|^2, \tag{39}$$

giving

$$\alpha^2 = \frac{2\|\mathbf{\Gamma}_1^w - \mathbf{\Gamma}_2^w\|^2}{(\boldsymbol{\gamma}_1^\top \boldsymbol{\gamma}_1 + \boldsymbol{\gamma}_2^\top \boldsymbol{\gamma}_2) + (\boldsymbol{\gamma}_1^\top \boldsymbol{\gamma}_1 - \boldsymbol{\gamma}_2^\top \boldsymbol{\gamma}_2)\cos(2\theta) + 2\boldsymbol{\gamma}_1^\top \boldsymbol{\gamma}_2 \sin(2\theta)}. \tag{40}$$

6 Additional Remarks

We plan to provide the Matlab source code for our pose estimation approach to the public once this paper gets accepted.

References

[1] S. Seitz, B. Curless, J. Diebel, D. Scharstein, and R. Szeliski. A comparison and evaluation of multi-view stereo reconstruction algorithms. In *CVPR'06*, pages 519–528. IEEE Computer Society, 2006. 1, 5